JOURNAL OF GEOPHYSICAL RESEARCH, VOL. 115, D05203, doi:10.1029/2009JD012864, 2010

Appearance of strong absorbers and fluorophores in limonene-O_3 secondary organic aerosol due to NH_4^+-mediated chemical aging over long time scales

David L. Bones,[1] Dana K. Henricksen,[1] Stephen A. Mang,[1] Michael Gonsior,[2] Adam P. Bateman,[1] Tran B. Nguyen,[1] William J. Cooper,[2] and Sergey A. Nizkorodov[1]

Received 21 July 2009; revised 1 October 2009; accepted 8 October 2009; published 6 March 2010.

[1] This study investigated long-term chemical aging of model biogenic secondary organic aerosol (SOA) prepared from the ozonolysis of terpenes. Techniques including electrospray ionization mass spectrometry (ESI-MS), UV-visible spectroscopy, Fourier transform infrared (FTIR) spectroscopy, NMR, and three-dimensional fluorescence were used to probe the changes in chemical composition of SOA collected by impaction on substrates and also of aqueous extracts of SOA. The addition of ammonium ions or amino acids to limonene SOA reproducibly produced orange-colored species that strongly absorbed visible radiation and fluoresced at UV and visible wavelengths. Simultaneous addition of H_2SO_4 to the SOA aqueous extracts inhibited this color transformation. These observations suggest the existence of aging processes leading to heavily conjugated molecules containing organic nitrogen. The presence of nitrogen in the chromophores was confirmed by the dependence of the absorption and fluorescence spectra on the amino acids added. In contrast to the strong change in the absorption and fluorescence spectra, there was no significant change in the ESI-MS, FTIR, and NMR spectra, suggesting that the chromophores were minor species in the aged SOA. Aqueous extracts of aged limonene + NH_4^+ SOA were characterized by an effective base-e absorption coefficient of $\sim$3 L g^{-1} cm^{-1} at 500 nm. Assuming particulate matter concentrations typical of polluted rural air gives an upper limit of 0.2 M m^{-1} for the aerosol absorption coefficient due to the aged limonene oxidation products. Biogenic SOA can therefore become weakly absorbing if they undergo aging in the presence of NH_4^+-containing aerosol.

Citation: Bones, D. L., D. K. Henricksen, S. A. Mang, M. Gonsior, A. P. Bateman, T. B. Nguyen, W. J. Cooper, and S. A. Nizkorodov (2010), Appearance of strong absorbers and fluorophores in limonene-O_3 secondary organic aerosol due to NH_4^+-mediated chemical aging over long time scales, *J. Geophys. Res.*, *115*, D05203, doi:10.1029/2009JD012864.

1. Introduction

[2] The contribution of aerosol to global climate change is still poorly understood; it represents the largest uncertainty in the current predictions of global warming models [*Forster et al.*, 2007]. Two effects, direct and indirect, dictate the net contribution of aerosol to radiative forcing. The indirect effect describes how aerosols affect the microphysical properties and distribution of clouds. Cloud droplets efficiently scatter light and hence have a negative net radiative forcing contribution. The direct effect is from absorption and scattering of light by the particles themselves. Much emphasis has historically been placed on the absorption of light by elemental carbon (operationally defined as "black carbon") [*Horvath*, 1993], but recently the potential for organic carbon as an absorber of UV and visible light ("brown carbon") has become clear [*Andreae and Gelencsér*, 2006; *Gelencsér et al.*, 2002; *Gelencsér et al.*, 2000; *Kirchstetter and Novakov*, 2004; *Moosmüller et al.*, 2009].

[3] Direct measurements of aerosol optical thickness (AOT) in combination with studies investigating the composition of atmospheric aerosol allow the estimation of the relative contributions to the overall absorption by elemental and organic carbon [*Hodzic et al.*, 2006; *Marley et al.*, 2009; *Yang et al.*, 2009]. A useful parameter to distinguish between these two classes of compounds is the absorption Ångström exponent (α), which describes the variation in absorption with wavelength [*Bergstrom et al.*, 2007; *Kirchstetter and Novakov*, 2004; *Marley et al.*, 2009]. In this model, the aerosol absorption coefficient β is represented as follows:

$$\beta = \beta_0 \cdot \lambda^{-\alpha},$$

where λ is the wavelength and β_0 is the aerosol absorption coefficient at a reference wavelength (e.g., 1 μm). The

[1]Department of Chemistry, University of California, Irvine, California, USA.
[2]Department of Civil and Environmental Engineering, University of California, Irvine, California, USA.

0148-0227/10/2009JD012864$09.00

refractive index of elemental carbon is relatively independent of wavelength because it absorbs all light indiscriminately, resulting in $\alpha = 1$ in the small particle limit and $\alpha = 0$ in the large particle limit [*Bergstrom*, 1972; *Bergstrom et al.*, 2002]. For particles dominated by organic compounds, α is typically higher because of electronic transitions in the UV-visible range. Typical values are $\alpha \sim 2$ and in some cases, such as the water soluble component of biomass burning aerosol, α can be as high as 6 or 7 [*Gelencsér et al.*, 2003; *Hoffer et al.*, 2006; *Kirchstetter and Novakov*, 2004; *Roden et al.*, 2006]. At short wavelengths, then, the contribution of organic carbon to AOT can be significant; on a global scale it is higher than the contribution from elemental carbon [*Tsigaridis et al.*, 2006].

[4] The identity of these absorbing organic compounds is as yet far from clear. A significant proportion (20–50%) of the water soluble organic components of aerosol have been classified as "humic-like substances" (HULIS), because their chemical properties are similar to that of humic acid [*Graber and Rudich*, 2006; *Limbeck et al.*, 2003; *Mukai and Ambe*, 1986; *Zappoli et al.*, 1999]. Humic-like substances arise from a variety of sources; particularly biomass burning [*Hoffer et al.*, 2006; *Lukács et al.*, 2007; *Reid et al.*, 2005] but also oxidation of biogenic terpenes [*Limbeck et al.*, 2003]. A closely linked class of compounds exists under the label of chromophoric dissolved organic matter (CDOM), a subset of the dissolved organic matter (DOM) extracted from terrestrial, marine and atmospheric waters [*Blough and Del Vecchio*, 2002]. CDOM shares many of the properties of HULIS in the sense that they both consist of heterogeneous, light absorbing, refractory and water soluble macromolecular substances [*Graber and Rudich*, 2006; *Santos et al.*, 2009]. "Atmospheric waters" containing CDOM include clouds and fogs that exist in a dynamic equilibrium with aerosols. Within this changing environment, a variety of aging processes are both oxidizing the organic components and catalyzing organic reactions, which may lead to macromolecular, aromatic CDOM and HULIS compounds [*Mukai and Ambe*, 1986].

[5] The chemistry producing these third-generation products in secondary organic aerosol will depend somewhat on the origin of the SOA, but in general two routes are likely. First, SOA constituents can react with oxidants (OH, O_3) or inorganic species (NH_4^+, H_2SO_4, etc.) present in the particles. An example of this kind of reaction leading to chromophoric species is the nitration of polycyclic aromatic hydrocarbons [*Jacobson*, 1999; *Kwamena and Abbatt*, 2008; *Pitts et al.*, 1978]. Proxies of SOA from biomass burning have been shown to form not only oligomers upon oxidation with OH [*Holmes and Petrucci*, 2007], but also colored products [*Gelencsér et al.*, 2003; *Hoffer et al.*, 2004]. Second, SOA constituents can undergo bond-forming reactions with other SOA constituents generating dimers and larger oligomers [*Kroll and Seinfeld*, 2008; *Rudich et al.*, 2007]. For example, acid catalyzed aldol condensation of volatile aldehydes to less volatile species has been suggested as a potential source of SOA, in addition to direct condensation of nonvolatile oxidation products [*Jang et al.*, 2002; *Zhang et al.*, 2002]. These condensation reactions may explain the higher than expected concentrations of SOA in the atmosphere [*Chen and Griffin*, 2005; *Volkamer et al.*, 2007]. Furthermore, some of the condensation products were observed to absorb radiation in the visible region [*Garland et al.*, 2006; *Nozière and Córdova*, 2008; *Nozière et al.*, 2007, 2009a; *Nozière and Esteve*, 2005; *Zhao et al.*, 2005]. Condensation reactions continue in the condensed phase as the aerosol ages, building macromolecules or oligomers out of monomeric units [*Barsanti and Pankow*, 2005; *Czoschke and Jang*, 2006a; *Li et al.*, 2008; *Zhao et al.*, 2005]. *Garland et al.* [2006] studied the reaction of gas phase hexanal with sulfuric acid and ammonium sulfate aerosols. They showed that dimerization, rather than more extensive polymerization, could account for much of the organic content of aerosol. Concentrated sulfuric acid has been shown to catalyze the self-condensation reaction of acetone to form trimethyl benzene via mesityl oxide [*Duncan et al.*, 1999], while the acid catalyzed condensation of acetaldehyde leads to chromophoric species [*Nozière et al.*, 2009a; *Nozière and Esteve*, 2005]. The increase in yield of SOA from terpene ozonolysis when acidic seed aerosols are added has been attributed to heterogeneous aldol condensation [*Czoschke and Jang*, 2006b; *Czoschke et al.*, 2003].

[6] Organic species containing multiple carbonyl groups are good candidates as building blocks for chromophoric compounds in aged SOA. Glyoxal, the simplest dicarbonyl and a gas phase compound under tropospheric conditions, has recently attracted attention as a potential source of highly oxidized oligomeric compounds in SOA [*Corrigan et al.*, 2008; *Kroll et al.*, 2005; *Kua et al.*, 2008; *Liggio et al.*, 2005]. A question of some contention is whether reactions of polycarbonyls are in fact more likely to be catalyzed by inorganic aerosol components other than sulfuric acid, by nitrogen containing compounds in particular [*De Haan et al.*, 2009; *Kroll et al.*, 2005; *Nozière et al.*, 2009a; *Peltier et al.*, 2007; *Volkamer et al.*, 2007]. Investigations observing the production of chromophores when ammonium ions are added to aqueous glyoxal suggested that the glyoxal reacts with the ammonia, formed upon dissociation of the NH_4^+ ion, to form imines which can then form conjugated species like imidazoles or highly oxygenated polymers [*Galloway et al.*, 2009; *Nozière et al.*, 2009b; *Shapiro et al.*, 2009]. De Haan et al. recently reported that such condensation reactions between glyoxal and amino acids lead to the appearance of products with characteristic brown color [*De Haan et al.*, 2009]. Given these observations, it seems likely that SOA generated from the ozonolysis of biogenic terpenes like limonene may contribute to atmospheric condensed phase "brown carbon."

[7] This study focused on the generation of chromophores induced by addition of ammonium ions and amino acids to biogenic secondary organic aerosol, primarily from oxidation of *d*-Limonene (1-methyl-4-(1-methylethenyl)-cyclohexene). Limonene accounts for up to 16% of monoterpene emissions on a global scale [*Kanakidou et al.*, 2005], and is a major source of secondary organic aerosol (SOA) via its reaction with ozone, OH and other free radicals. Several groups have studied the composition of SOA prepared by ozonolysis of limonene [*Bateman et al.*, 2009; *Glasius et al.*, 2000; *Heaton et al.*, 2007; *Jaoui et al.*, 2006; *Leungsakul et al.*, 2005; *Ng et al.*, 2006; *Walser et al.*, 2008; *Zhang et al.*, 2006]. Reactions between limonene ozonolysis products and NH_4^+ are likely because they are rich in carbonyl groups

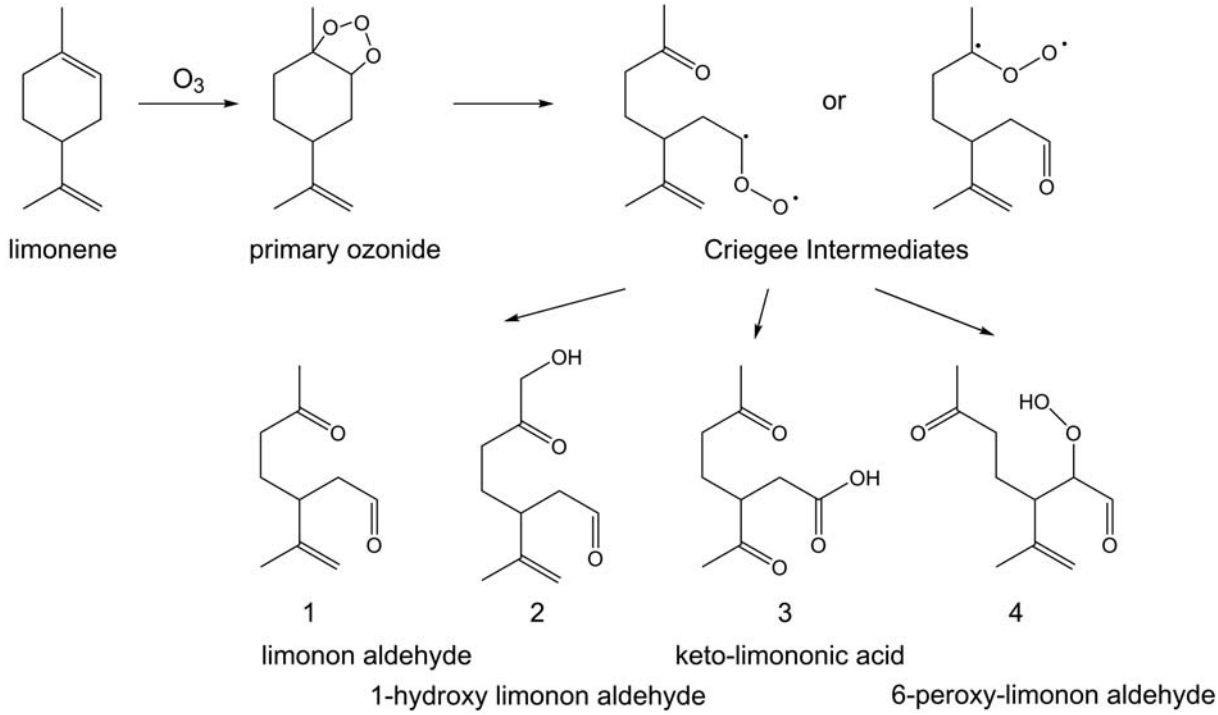

Figure 1. Representative products of limonene ozonolysis. Product names are based on the scheme suggested by *Larsen et al.* [1998]. Note the prevalence of carbonyl functional groups among the products.

[*Bateman et al.*, 2009; *Glasius et al.*, 2000; *Jaoui et al.*, 2006; *Leungsakul et al.*, 2005; *Mang et al.*, 2008]. Ozone adds across the endocyclic bond in limonene to form primary ozonides (POZ) which decompose to form Criegee intermediates and then react further to form a plethora of oxidized compounds (Figure 1) [*Kroll and Seinfeld*, 2008]. The less volatile compounds quickly condense to form SOA [*Griesbaum et al.*, 1996; *Jaoui et al.*, 2006; *Jonsson et al.*, 2008; *Leungsakul et al.*, 2005]. Typically, the reaction products are multifunctional organic acids (e.g., compound 3) and carbonyl containing compounds (1–4). Secondary ozonides and other types of peroxides (compound 4) are also common. The endocyclic double bond reacts 10 to 50 times faster with ozone than the exocyclic double bond [*Zhang et al.*, 2006], hence many of the products lack the six-membered ring of limonene but still retain a branched C_{10} carbon backbone and a terminal double bond [*Griesbaum et al.*, 1996; *Jaoui et al.*, 2006].

[8] The color change processes discussed in this paper take place over considerably longer time scales (days) than afforded by typical chamber measurements (hours). This necessitates studying the time-dependent composition of SOA that was collected on filters or impactors. "Aged SOA" in this context means SOA that has been collected on a nonreactive substrate and left for days after addition of ammonium sulfate. Because of the constant variations in relative humidity in the atmosphere, SOA always contain some amount of adsorbed water. SOA can nucleate cloud/fog droplets under supersaturated conditions. Therefore, aging of aqueous extracts of SOA is also studied in this work. "Aged SOA extract" in this context means an SOA sample dissolved in water and left in the solution in the presence of various additives, such as amino acids, salts, H_2SO_4, etc.

2. Experimental Setup

2.1. Particle Generation and Collection

[9] SOA was produced from the reaction of *d*-limonene and other terpenes with ozone in a 17 L glass flow tube at ambient atmospheric pressure (750 ± 10 Torr), low relative humidity (<2%) and ambient temperature (295 ± 2 K). The flow tube was covered so that the oxidation reaction proceeded in the dark. The *d*-limonene was introduced into a flow of zero air and ozone via a syringe pump (Fisher, KDS100) at a rate of 20 μL h^{-1}. The concentration of terpene was controlled by varying the flow rates and the syringe pump speed. Zero air was supplied by a purge gas generator (Parker 75–62), while ozone was produced by flowing oxygen gas (99.994% purity) through a commercial ozone generator. A large excess of ozone was used in order to improve SOA yield. OH-radical scavengers were not used. At typical flow rates, the reactants were in the flow tube for 4 min, with concentrations of 20 ppm and 10 ppm for ozone and terpene, respectively. Lower reagent concentrations (2 ppm ozone, 400 ppb limonene) were also used to ensure that the experimental observations were not strongly concentration dependent. The latter set of concentrations is equivalent to exposure of limonene to 100 ppb ozone for 80 min; this level of exposure is similar to those encountered during oxidation of limonene in polluted air masses. The ozone concentration was measured spectrophotometrically from the absorption of the 254 nm Hg line in a home-built

quartz flow cell of known path length. After the flow tube, the resulting mixture flowed through a denuder filled with activated charcoal where excess ozone and some volatile organic compounds were removed before the SOA was collected via a 10 stage cascade impactor (MOUDI 100, MSP). Depending on the analysis, different substrates were used including aluminum foil for ESI-MS, NMR and aqueous phase UV-visible spectroscopy, calcium fluoride windows for UV-visible spectroscopy or zinc selenide windows for FTIR spectroscopy. Experiments typically involved 2 h of SOA collection. The 10 rotating stages of the impactor deposit the aerosol particles fairly uniformly on the substrate. While this impactor is designed to classify the aerosol based on particle diameter, the samples from the various stages were typically combined when the SOA was extracted in water or chloroform. Ammonium sulfate aerosol was generated with a medical nebulizer (SPAG-2 6000, ICN Pharmaceuticals) and was either used to seed SOA generation or sprayed onto samples after the SOA had been collected. For comparison purposes, some experiments were also performed in static 200–300 L Teflon chambers as described previously [*Mang et al.*, 2008; *Walser et al.*, 2008]. The substrates were weighed to ±2 μg accuracy before and after collection using an analytical microbalance (Sartorius ME-5F) in order to determine the mass of SOA collected.

2.2. Sample Analysis

[10] UV-visible spectroscopy of collected SOA material was conducted with the impaction windows placed in a custom-made sample holder that held them on either side of a sealed glass flow cell, thus enabling long-term exposure to gas flow with controlled composition and humidity. Spectra were collected in a dual-beam spectrometer (Shimadzu Model 2450), using two clean CaF_2 windows as reference. UV spectra were recorded immediately after particle collection and for a period of up to 72 h afterward. The samples were aged in darkness using a humidified flow of zero air (50 to 60 RH%).

[11] In a separate set of experiments, the SOA samples were dissolved in distilled water whereupon various compounds were added to the solution. Compounds added included ammonium sulfate, the amino acids glycine, arginine, cysteine and alanine, sulfuric acid and sodium chloride. The addition of sulfuric acid enabled the reaction to be studied at lower pH values. The solutions were filtered (nylon 0.2 μm filter, Acrodisk) then placed in a quartz cuvette of 10 mm path length for the absorption measurements. Absorption spectra were measured at hourly intervals for 20 h as the solution aged. The sample remained in the cuvette for the duration of the aging experiment. The cuvette was exposed to a negligibly small flux of 700 nm radiation from the spectrometer in between the scans.

[12] Aqueous samples, prepared as for UV-visible spectroscopy, were analyzed by three-dimensional excitation emission matrix (EEM) fluorescence spectroscopy (Fluoromax-4, Horiba Jobin Yvon). Excitation wavelengths from 240 to 500 nm at 5 nm intervals irradiated the sample while a detector at 90° to the excitation beam measured the emission spectra from 300 to 600 nm. The slit widths were held constant for excitation and emission at an effective bandwidth of 5 nm. The resulting EEM were corrected for Raleigh and Raman scattering peaks and calibrated relative to quinine sulfate equivalent (QSE) units using a Matlab toolbox (FLtoolbox 1.91) developed by *Zepp et al.* [2004].

[13] Electrospray ionization mass spectrometry (ESI-MS) was used to analyze the molecular mass distribution of SOA components before and after aging. Aqueous solutions of SOA were ionized using the positive ion mode (Micromass LCT). Where necessary, HPLC was used to separate the excess NH_4^+, SO_4^{2-} and other inorganic ions from the organic compounds to avoid domination of the mass spectra by inorganic clusters.

[14] Samples were dissolved with chloroform-d for NMR analysis on a Bruker DRX500 spectrometer with TCI cryoprobe. A combination of ^{1}H-NMR, ^{13}C-NMR, HMQC (2-D proton-carbon coupling) and COSY (2-D proton-proton coupling) aided in assignment of functional groups in SOA samples.

[15] Finally, SOA samples collected on ZnSe windows were analyzed by FTIR spectroscopy (Galaxy 5000, Mattson) before and after aging. The procedure was similar to that for measuring UV-visible spectra of films of SOA material. Spectra were collected relative to clean ZnSe windows. The sample compartment was purged with zero air from a purge gas generator.

3. Results

3.1. UV-Visible Spectroscopy

[16] A reproducible color change from colorless to orange was observed whenever aerosols containing ammonium ions were sprayed onto a film of collected limonene SOA or $(NH_4)_2SO_4$ aerosol was used as a seed particle for limonene SOA condensation. Corresponding absorption maxima appeared at 430 nm and 505 nm over hours or days (Figure 2c). In the absence of NH_4^+ the only spectral change noticed was a change in absorbance in the vicinity of 250 nm.

[17] The spectral change was evident not only for limonene SOA films exposed to ammonium sulfate aerosol but also for limonene SOA samples that were generated without any seed particles and then dissolved in aqueous, non-acidified solutions containing $(NH_4)_2SO_4$ (Figures 2a, 2b, and 3). At pH < 5, the color change was inhibited (see auxiliary material Figure S1) in agreement with previous studies of glyoxal + NH_4^+ reactions by *Nozière et al.* [2009b], which showed that NH_4^+ + carbonyl chemistry occurs over a relatively narrow pH range (although *Shapiro et al.* [2009] observed visible light absorbing compounds from glyoxal + NH_4^+ reactions at pH = 4).[1] Sulfuric acid alone was not sufficient to catalyze the formation of any chromophores from limonene SOA but a slow rise in absorption at 505 nm was still observed at pH > 4 as long as some NH_4^+ was present. Addition of sodium chloride to limonene SOA solutions did not result in visible color change (Figure 2d).

[18] Addition of amino acids (glycine, alanine, arginine and cysteine) to aqueous solutions of limonene SOA produced similar absorption peaks, red-shifted by different amounts relative to the SOA+NH_4^+ absorption peaks (Figure 2e). This can be taken as direct evidence that the chromophore includes nitrogen from the amine group and that this functional group is part of the chromophore. Addition of cysteine produced an

[1] Auxiliary materials are available in the HTML. doi:10.1029/2009JD012864.

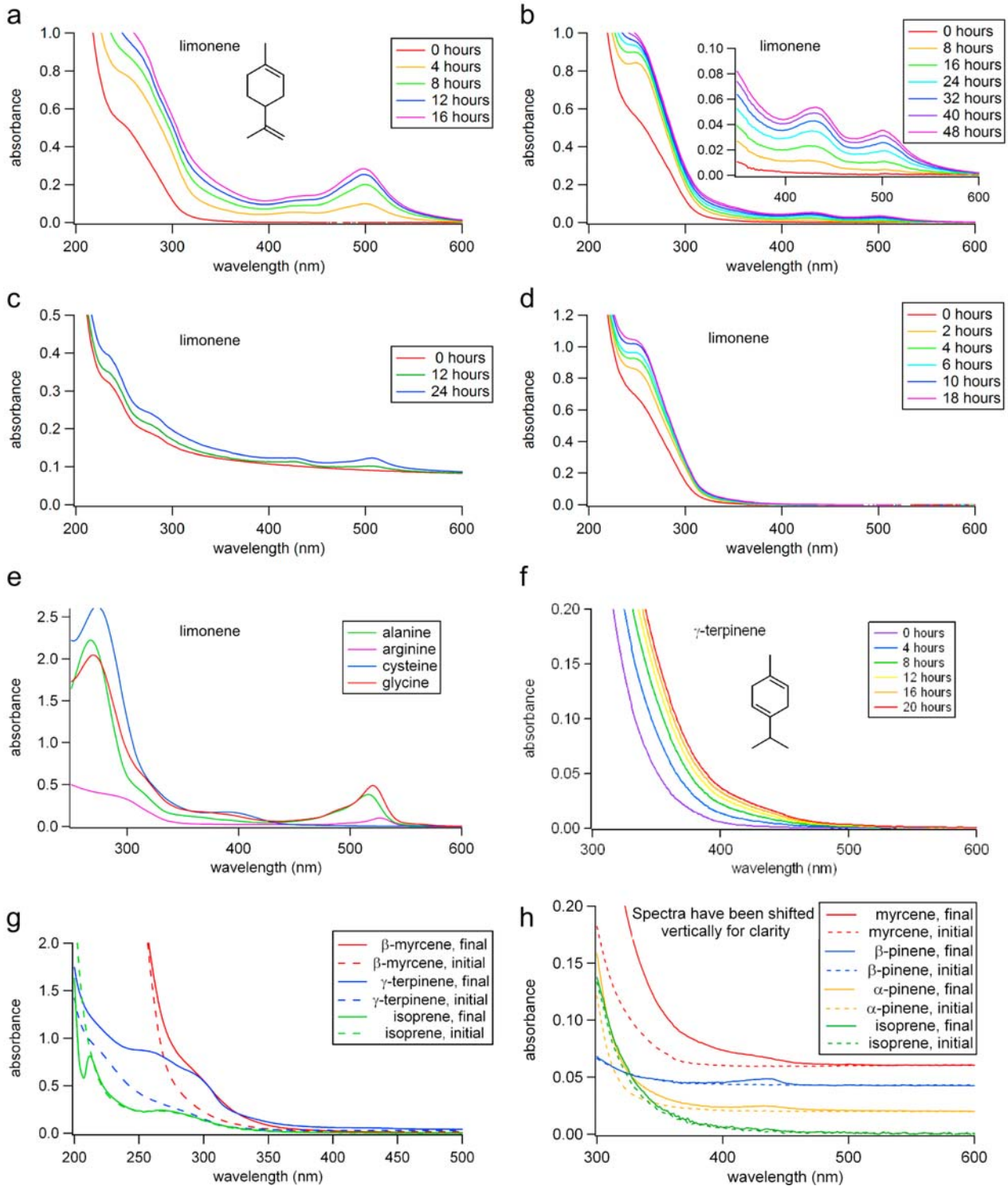

Figure 2. UV-visible absorption spectra of limonene SOA. All measurements were conducted in aqueous solutions (10 mm path length) unless indicated otherwise. (a) Limonene SOA + H_2O + excess $(NH_4)_2SO_4$; (b) excess limonene SOA + H_2O + $(NH_4)_2SO_4$; (c) limonene SOA on CaF_2 window, sprayed with $(NH_4)_2SO_4$ aerosol; (d) limonene SOA + H_2O + NaCl; (e) limonene SOA + various amino acids + H_2O; (f) SOA from γ-terpinene + $(NH_4)_2SO_4$ + H_2O; (g) SOA from other terpenes + $(NH_4)_2SO_4$ + H_2O; and (h) SOA from other terpenes + $(NH_4)_2SO_4$ + H_2O (expanded view).

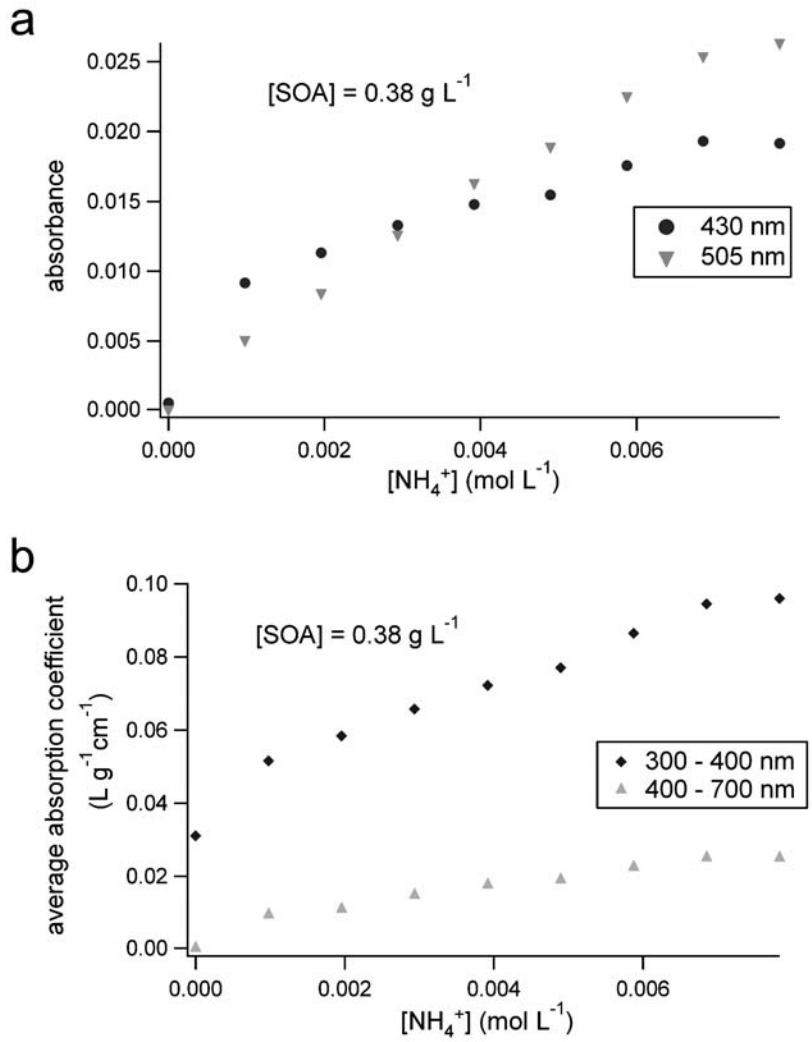

Figure 3. Absorption increases (base-10) with increasing concentrations of NH_4^+, for fixed limonene SOA concentration (0.38 g L^{-1}). Limonene SOA extracts were aged for 20 h. (a) The chromophores responsible for the two absorption maxima (at 430 nm and 505 nm) do not appear simultaneously. (b) Total absorption increases fairly steadily with NH_4^+ concentration for both the near UV region (300–400 nm) and the visible region (400–700 nm).

absorption maximum at 400 nm. Cysteine is a unique amino acid that has a thiol group that could influence the electronic structure of the chromophore resulting from the reaction with the SOA or form a chemically distinct chromophore as a result of thiol-specific chemistry.

[19] SOA produced from other terpenes (β-myrcene, isoprene, α-pinene and β-pinene) did not exhibit significant color change in the visible region upon mixing with NH_4^+, but absorption in the UV region changed (Figures 2g, 2h, and 4). The γ-terpinene was an exception, with absorption extending from the UV region out to 500 nm. This is noteworthy because γ-terpinene, of the terpenes tested, has the structure most similar to limonene. To compare the total absorption across relevant regions of the UV-visible spectrum, absorbance was averaged across the visible region (400–700 nm) and the near ultraviolet region (300–400 nm) of the spectra (Figure 4). In each case, the averaged absorbance was converted to an absorption coefficient by dividing by the concentration of SOA, in grams per liter, and the path length. These calculations assume that all of the collected SOA was fully extracted into the aqueous phase.

[20] No color change was observed in any experiment if water was not present as either solvent or humidified air. The absorption at 250 nm increased significantly for all aqueous solutions of dissolved SOA (with or without added NH_4^+ or amino acids). In the absence of water, absorption in the UV actually decreased for SOA collected on windows, most likely due to slow evaporation of semivolatile organics.

[21] We confirmed that the observed color change was not caused by an impurity in limonene, such as tocopherol (vitamin E) which is frequently added to monoterpenes as a stabilizer. For example, no color change was observed in experiments in which SOA was prepared from myrcene purposefully mixed with tocopherol. Experiments using monoterpenes that were purified by vacuum distillation gave the same results as experiments using chemicals as obtained from the manufacturers.

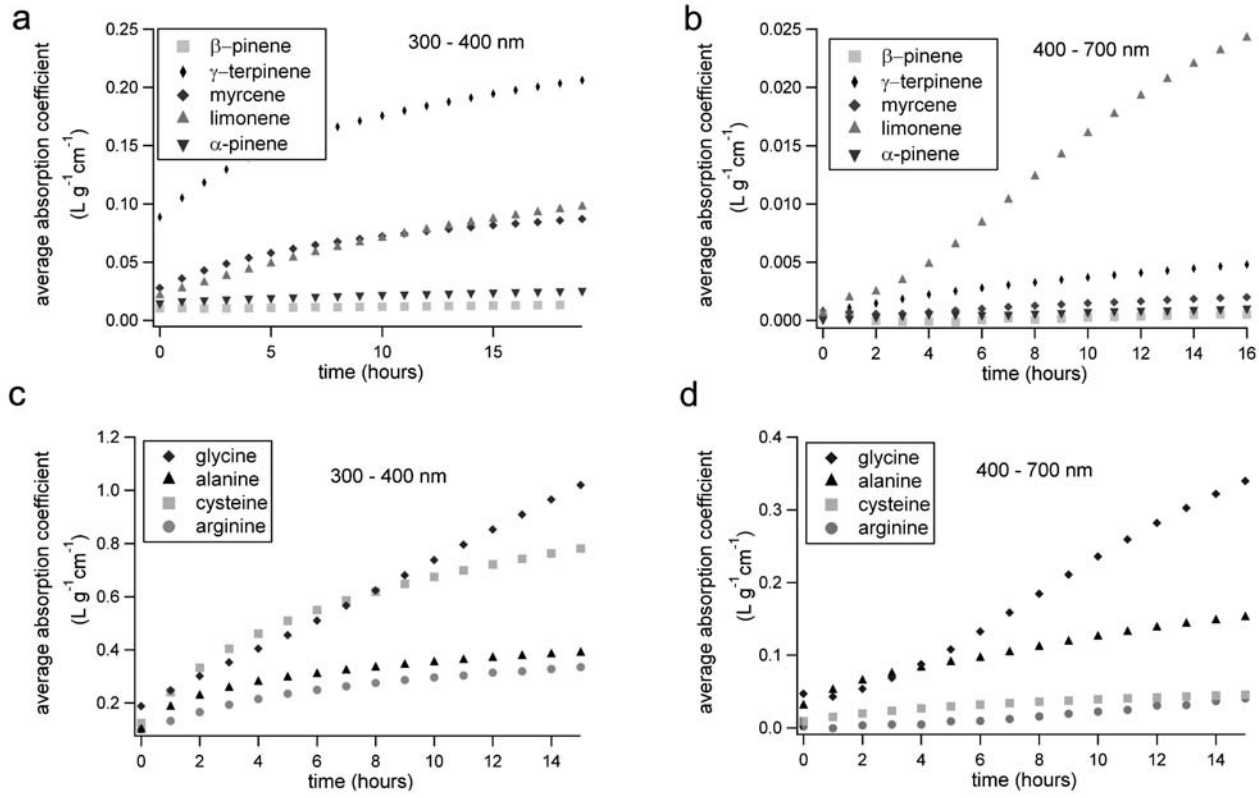

Figure 4. The increase in the average absorption coefficients (base 10) over time for aqueous extracts of SOA from different terpenes treated with NH_4^+: (a) average over 300 to 400 nm (the near ultraviolet) and (b) average over 400 to 700 nm (the visible range). Similarly for aqueous extracts of limonene SOA treated with various amino acids: (c) 300 to 400 nm and (d) 400 to 700 nm.

[22] Care was taken to filter solutions before UV-visible absorption measurements. Unfiltered extracts contained sufficient numbers of undissolved particles to produce a small but noticeable wavelength independent contribution to the measured "absorption" from scattered light. This scattering background decreased over hours and disappeared as the particles fully dissolved. Filtered extracts did not exhibit this phenomenon. It is unlikely that formation of colloids during aging contributed much to the increase in absorption of the treated SOA extracts. First, the increase in absorption was at specific wavelengths and second, aged SOA samples on foil substrates exhibited very similar absorption maxima in various solvents: water, isopropyl alcohol, acetonitrile and $CDCl_3$. We confirmed that the formation of colloidal particles was insignificant using Dynamic Light Scattering (Zetasizer Nano, Malvern Instruments); counts proved to be at the limit of detection of the instrument, on the order of those measured for AR grade water.

3.2. Other Analyses

[23] Limonene SOA samples treated with NH_4^+ or amino acids were observed to fluoresce strongly (Figure 5). The addition of NH_4^+ resulted in up to 3 peaks in the excitation-emission plots whose intensities varied with the ratio of NH_4^+ to SOA. An intense fluorophore was also formed when glycine was added to limonene SOA, with an emission band at 400 nm (Figure 5e). The addition of cysteine and alanine to limonene SOA also resulted in fluorescence peaks (auxiliary material Figure S2). Imine compounds, which are the suspected products of the polycarbonyl+NH_4^+ reactions, are known to form fluorescent chromophores with emission bands at visible wavelengths; for example, the di-imine formed from the reaction of malonaldehyde with two molecules of glycine (Figure 6) fluoresces at 430 to 490 nm [*Chio and Tappel*, 1969]. In general, fluorescence at longer wavelengths is attributed to a high degree of aromaticity or highly functionalized compounds [*Kieber et al.*, 2006; *Santos et al.*, 2009]. Aqueous extracts of γ-terpinene SOA and myrcene SOA also fluoresced strongly at 400 nm when aged in the presence of NH_4^+; other terpenes fluoresced predominantly in the UV region (auxiliary material Figure S2).

[24] The mass spectra for fresh and chemically aged (i.e., with NH_4^+) limonene-O_3 SOA were surprisingly similar (Figure 7, also auxiliary material Figure S3). The spectra were also similar to those previously reported for limonene-O_3 SOA, with peaks separated in several groups corresponding to monomeric, dimeric and trimeric products [*Bateman et al.*, 2009; *Walser et al.*, 2008]. FTIR spectra of fresh and aged limonene-O_3 SOA also showed few differences (auxiliary material Figure S4). The ESI-MS and FTIR results suggest that the aging chemistry leading to the observed color change is a relatively minor process that does not significantly change the average chemical make-up of SOA and does not lead to significant oligomerization.

[25] The small scale of the chemical changes due to SOA aging also resulted in similar NMR spectra for fresh

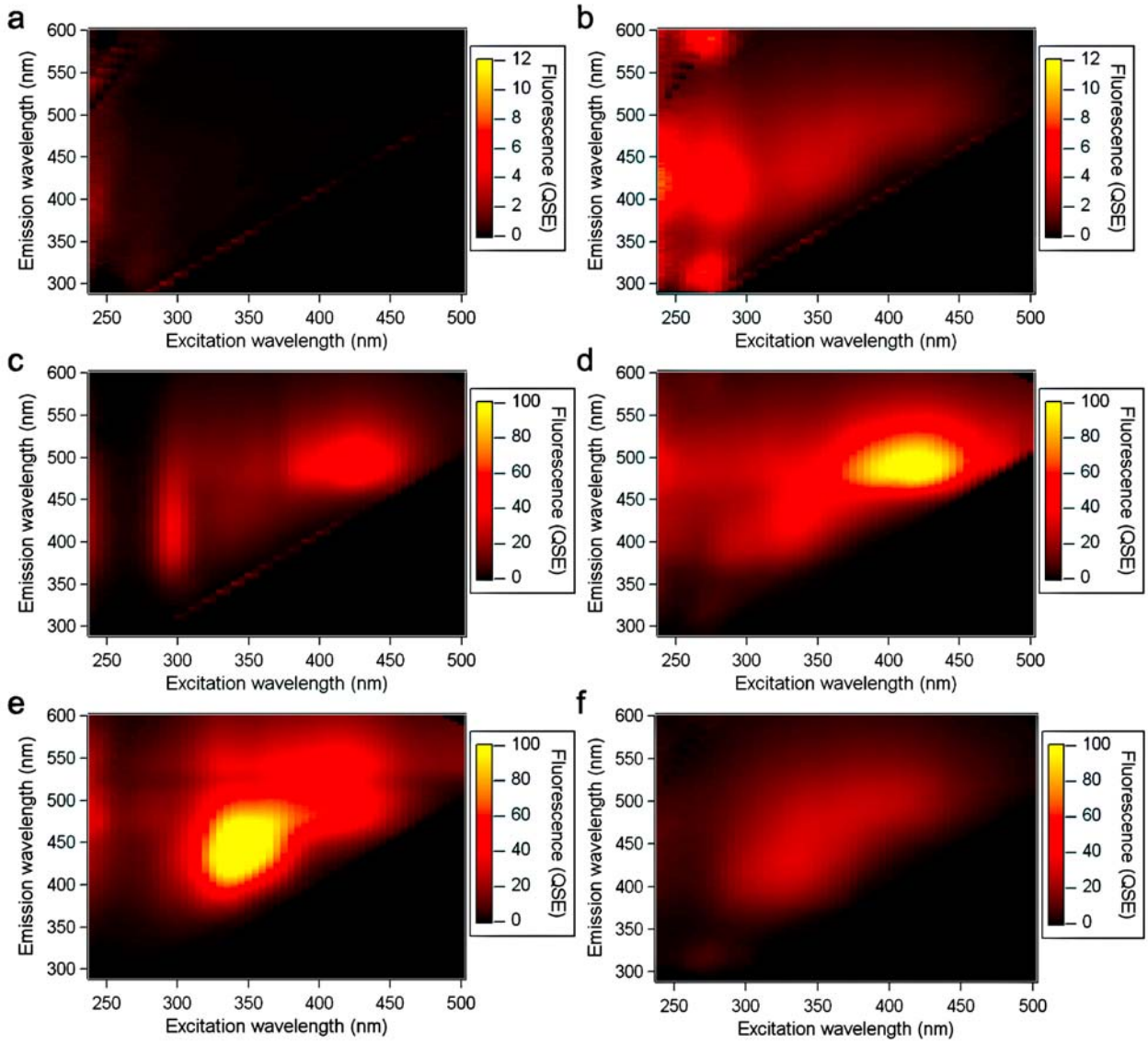

Figure 5. Three-dimensional fluorescence excitation-emission spectra of terpene SOA samples extracted into water. Note the different scales (color coded): (a) fresh limonene SOA; (b) 24 h aged limonene SOA (no NH_4^+); (c) NH_4^+ + excess limonene SOA; (d) limonene SOA + excess NH_4^+; (e) glycine + excess limonene SOA; and (f) γ-terpinene SOA + excess NH_4^+.

and aged limonene-O_3 SOA (Figure 8). Prominent peaks assigned in the 2-D HMQC NMR (proton-carbon correlations) corresponded to the exocyclic ''isopropylene'' double bond (4.8 ppm), acetal and/or secondary ozonide functionalities (5–6 ppm and 3.5–4.5 ppm) as well as many unresolved alkyl peaks (1–2 ppm) (auxiliary material Figures S5 and S6). Small differences were apparent: the peaks corresponding to aldehydes (9–10 ppm) were lower in intensity for chemically aged SOA spectra and the prominent peaks of the exocyclic double bond were also seen to decrease in intensity as the SOA aged. In order to collect ^{13}C-NMR (and hence HMQC), large amounts of sample (several milligrams) were required. The long collection time needed for 2-D NMR analysis (~6 h) may have affected the aging reactions and therefore, in terms of observable trends, the ^{1}H-NMR spectra are considered more reliable. The disappearance of the exocyclic double bond is noteworthy because this feature distinguishes limonene from most other cyclic terpenes. No peaks were seen in regions associated with aromaticity in the 2-D NMR spectra for either fresh or aged SOA.

4. Discussion

4.1. Mechanism

[26] The first question we need to address is whether acid-catalyzed aldol condensation, which is frequently quoted in the organic aerosol literature as a common oligomerization process [*Barsanti and Pankow*, 2005; *Czoschke and Jang*, 2006a; *Li et al.*, 2008; *Zhao et al.*, 2005], can be held responsible for the appearance of strong chromophores in aged SOA. Aldol condensation can occur in the SOA

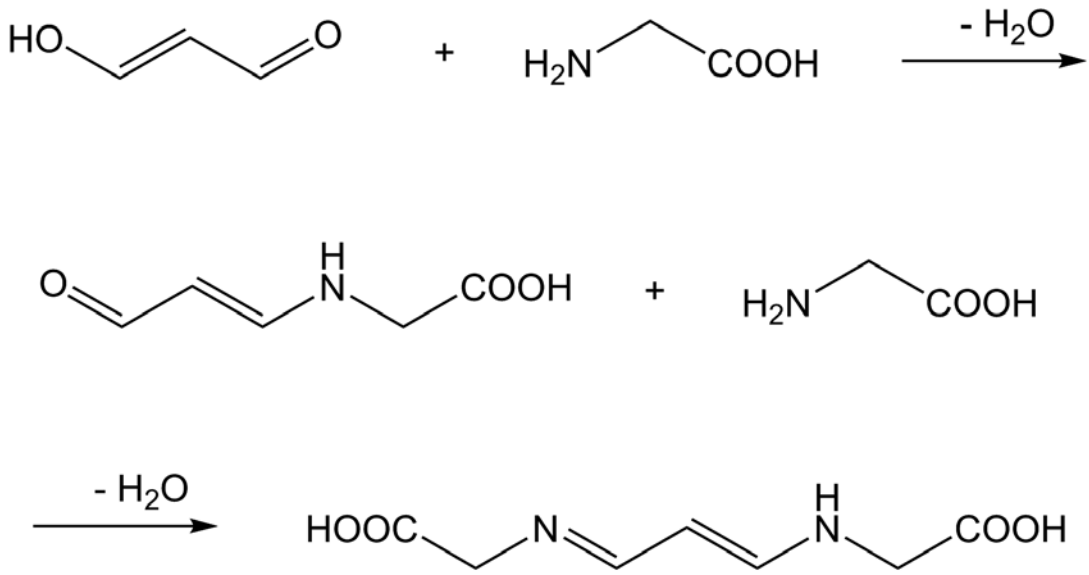

Figure 6. Example of a reaction between an amino acid (glycine) with an aldehyde (malonaldehyde) resulting in a highly fluorescent, nonaromatic compound containing C=N bonds. Malonaldehyde is functionally a dialdehyde but exists mainly in the enol form, as depicted here.

produced by ozonolysis of terpenes [*Iinuma et al.*, 2004; *Tolocka et al.*, 2004]. It can be catalyzed by acid, base or inorganic salts but requires an appropriate solvent, e.g., water. All of the aqueous solutions of SOA showed a rapid change in absorption at 250 nm which likely corresponds to an acid-catalyzed aldol condensation reaction. This reaction was slower for SOA particles collected on windows and exposed to humidified air because in this case the only water present was due to uptake of water by the particles. Aldol condensation is also consistent with the disappearance of peaks attributable to aldehydes in NMR spectra of aged SOA. However, aldol condensation is unlikely to be an important mechanism in the production of the strong visible chromophores since the degree of conjugation resulting from such reactions is insufficient to explain visible absorption. Even at the low pH conditions studied by *Casale et al.* [2007] and

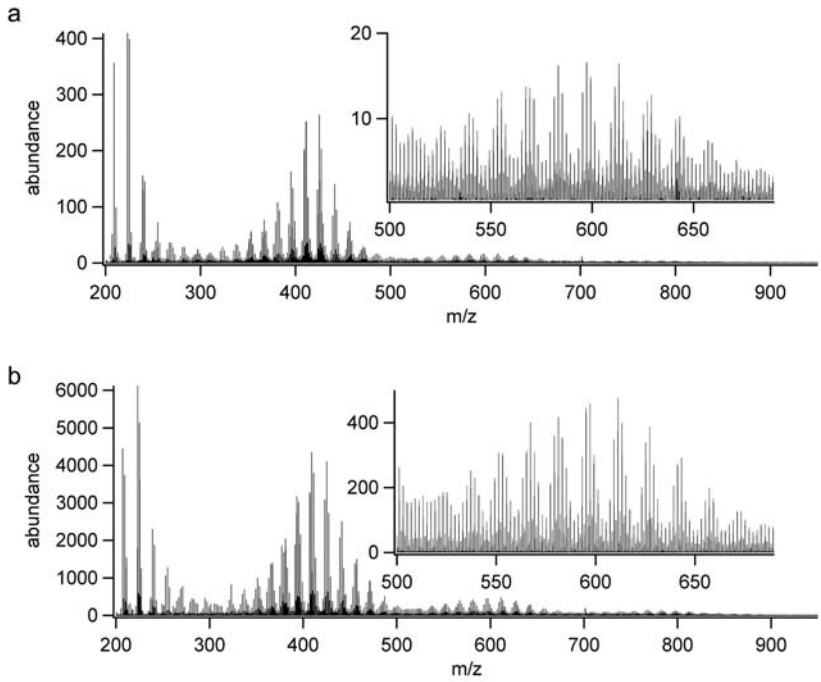

Figure 7. Electrospray ionization mass spectra of (a) fresh limonene SOA and (b) limonene SOA + NH_4^+, aged 24 h and processed with HPLC to remove excess NH_4^+. The similarity of these mass spectra strongly suggests that the absorbing species are minor components of SOA. See also auxiliary material Figure S3.

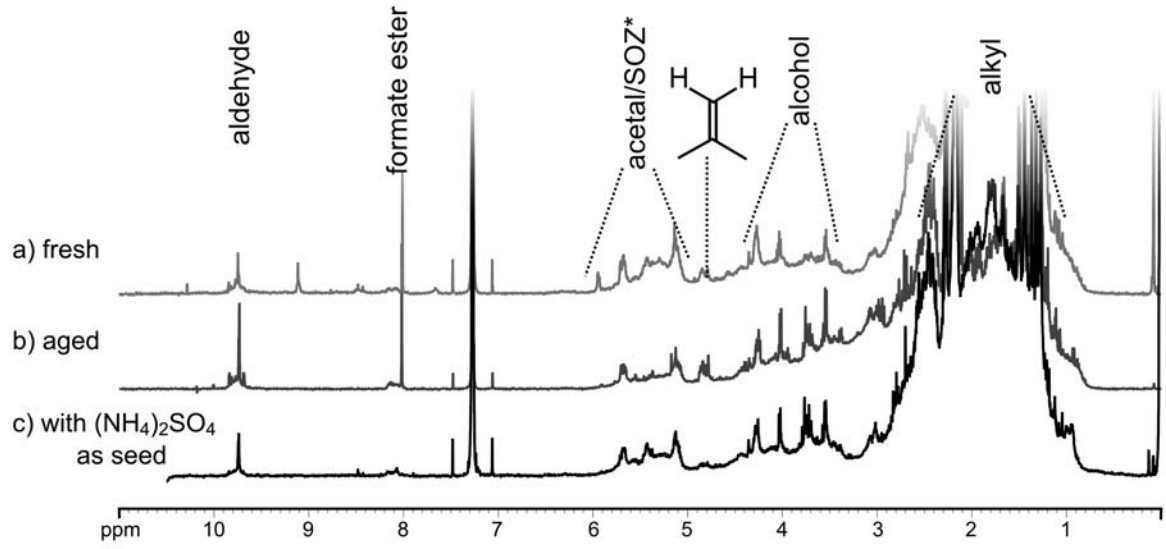

Figure 8. The ^{1}H-NMR spectra of fresh limonene-O_3 SOA (curve a); SOA aged without NH_4^+ (curve b); and SOA aged in the presence of NH_4^+ (curve c). Approximate functional group assignments are based on cross correlations in ^{1}H-^{13}C NMR spectra (see auxiliary material Figures S5 and S6). SOZ denotes secondary ozononide.

Garland et al. [2006], the absorption of aldol condensates of simple aldehydes in the visible region was limited to a tail stretching from peaks in the near-UV region.

[27] The absorption profile observed in this work is more consistent with the reaction of an ammonium ion with an aldehyde or ketone from limonene ozonolysis. The two prominent UV-visible absorption peaks at 430 and 505 nm appear at different times, are favored at different pH and are differently dependent on SOA and ammonium concentrations (Figure 3; see also auxiliary material Figure S1). This suggests that the 505 nm absorber is a different species from the 430 nm absorbing species, possibly produced by quite different chemistry. The peak at 430 nm dominates at high pH and at low ammonium concentrations. Amines are known to react with aldehydes via the Leuckart reaction to form an imine and/or an enamine [*Lawrence*, 2004]. This imine can then react via the Mannich Reaction to form a conjugated product, recycling the ammonium ion (Figure 9). A similar reaction has been proposed to explain the catalysis of glyoxal oligomerization by ammonia [*Nozière et al.*, 2009b].

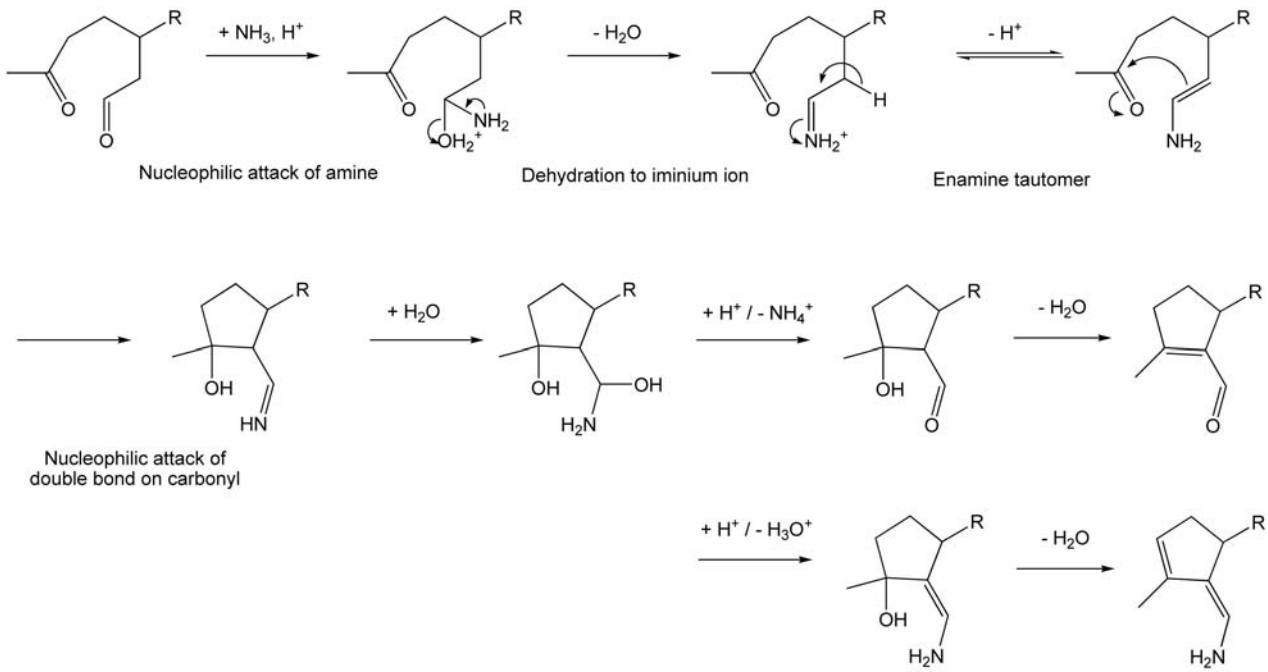

Figure 9. Examples of Leuckart and Mannich reactions involving a typical 1,6-dicarbonyl limonene ozonolysis product.

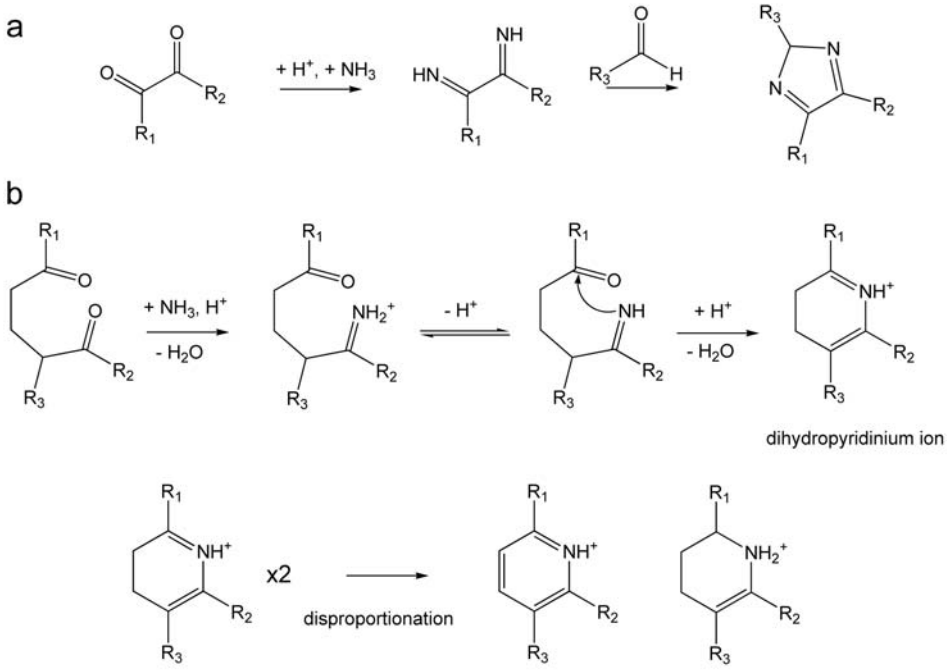

Figure 10. (a) Generalized Debus mechanism generating an imidazole ring from reaction of ammonia with a 1,2-dicarbonyl and a monocarbonyl compound and (b) 1,5-dicarbonyl reacting with ammonia then cyclizing to give a dihydropyridinium ion, which can then combine with another dihydropyridinium ion and disproportionate to give an aromatic pyridinium ion.

[28] The Leuckart and Mannich reactions can only occur within a fairly narrow pH window, as nucleophilic attack requires a lone pair of electrons on the nitrogen atom and hence basic conditions, while the dehydration step is acid catalyzed. Under highly acidic conditions, the formation of α,β unsaturated carbonyl species via aldol condensation is irreversible [*Casale et al.*, 2007]. If the aldehyde (or ketone) involved in the Leuckart reaction has an α-hydrogen atom, the iminium ion can tautomerize to an enamine, resulting in a C=C as opposed to a C=N double bond. The distribution of the double bonds in the chromophore will therefore depend on the relative stabilities of its tautomers; the more conjugated tautomers will be more stable.

[29] It is not obvious, however, whether the conjugation arising from the Leuckart/Mannich reaction mechanism is sufficient to produce chromophoric compounds. Formation of aromatic heterocyclic compounds from intermediate imine species represents the most likely explanation for the observed color change processes. For example, glyoxal has been reported to form an imidazole in the presence of NH_3 [*Galloway et al.*, 2008]. This reaction, first reported by *Debus* [1858] creates two neighboring imines that then react with an aldehyde to form the imidazole (Figure 10a). This reaction is unlikely in the case of limonene-O_3 SOA, however, since it requires neighboring carbonyl groups, a feature not typical in limonene ozonolysis products. Also, although conjugated, most imidazoles are colorless. A reaction with more potential for generation of chromophores involves a 1,5-dicarbonyl limonene SOA product reacting with NH_4^+ to form an imine which can then cyclize to form, upon the loss of a water molecule, a dihydropyridinium ion (Figure 10b) [*Eisner and Kuthan*, 1972; *Katritzky et al.*, 1986]. If two of these ions combine they can undergo disproportionation to form a substituted pyridinium ion, which would likely be sufficiently conjugated to absorb visible light. Such 1,5-dicarbonyl compounds are always present in limonene-O_3 SOA. Although the exocyclic double bonds react much slower with ozone than the endocyclic double bond, a significant percentage of the products are 1,5 dicarbonyl compounds as a result of having both bonds oxidized by ozone [*Glasius et al.*, 2000; *Jaoui et al.*, 2006], particularly so at the elevated concentrations of reactants used here.

[30] Evidence for the incorporation of nitrogen in the chromophore is clear from the observation that amino acids generate similar but not identical chromophores and fluorophores (Figures 2e and 5e and auxiliary material Figure S2). Amino acids can react with aldehydes in an analogous manner to the reaction between ammonia and aldehydes. Indeed, amino acids with simple structures like glycine and alanine resulted in chromophores with strong absorption peaks between 500 and 520 nm, while more substituted amino acids either produced chromophores with weaker absorption peaks (in the case of arginine) or peaks in different regions of the UV-visible spectrum altogether (in the case of cysteine). Reactions of acetaldehyde with various amino acids are known to produce a variety of condensation products absorbing mainly in the UV region [*Nozière et al.*, 2007]. Of the amino acids reacted with acetaldehyde, only arginine produced chromophores that absorbed in the visible region. Reactions between amino acids and glyoxal, however, have been observed to produce visible light absorbing species [*De Haan et al.*, 2009]. These were elucidated to be imidazole containing compounds formed from dimerization of the initial imine product.

4.2. Atmospheric Implications

[31] Laboratory studies of SOA are often rightfully criticized for using nonrealistic concentrations of oxidants and aerosol precursors in order to get sufficient quantities of SOA material for chemical analysis [*Barsanti and Pankow*, 2005; *Shilling et al.*, 2009]. At the ppm-level precursor and oxidant concentrations used in these experiments, it is possible that volatile compounds are also condensing onto the nonvolatile ozonolysis products. However, this effect is mitigated for three reasons. First, the exposure level, $[O_3] \times$ contact time, approaches that of the actual atmosphere. Furthermore, the combination of a denuder and impactor for the SOA collection makes it possible for the most volatile species to desorb from the SOA back into the gas flow before the aging begins. Finally, aldehydes such as compound 3 in Figure 1 are expected to have low vapor pressures and to hence be present both at the exaggerated concentrations of the flow tube experiments and in realistic atmospheric conditions. Highly oxidized compounds such as compound 3, particularly ones with carbonyl groups at 1,5 positions, are the most likely candidates for forming highly conjugated pyridine compounds with ammonia. We have observed similar color changes when O_3 and limonene concentrations were reduced by an order of magnitude each.

[32] Biogenic SOA is normally treated as a nonabsorbing, predominantly scattering aerosol [*Dinar et al.*, 2008]. In order to see whether the extent of the observed color change can convert biogenic SOA into an efficient light absorber, an estimate of the aerosol absorption coefficient is needed. This was obtained for aqueous extracts of aged SOA. A typical concentration of SOA in aqueous extract was 1.0 g L^{-1}, which upon treatment with excess NH_4^+ resulted in a maximum base-e absorbance of 0.7 at 500 nm after 1 day of reaction (path length = 10 mm). Assuming that Beer's law holds, we get a base-e mass absorption coefficient of 0.7 L g^{-1} cm^{-1} or 7×10^{-4} cm^2 μg^{-1}.

[33] Is this absorption coefficient significant? If we assume aerosol concentrations of 20 μg m^{-3} of which 25% is organic carbon [*Molnár and Mészáros*, 2001], the resultant aerosol absorption coefficient (β) is 0.3×10^{-6} m^{-1}. This calculation assumes that 100% of the organic fraction is derived from limonene. Although limonene does contribute a sizable portion of the organic component, especially in tropical regions, this is clearly an overestimation. Given that limonene represents up to 16% of reactive organic compounds (as a global average) [*Kanakidou et al.*, 2005], an aerosol absorption coefficient of 0.06×10^{-6} m^{-1} may be a more realistic estimate for the aged biogenic SOA. An implicit but realistic assumption is that the aerosol particles will have NH_4^+ concentrations in excess of the concentrations of the reactive SOA components, and that sufficient levels of water vapor will be present to drive the reactions. Films of limonene-O_3 SOA collected on windows aged more slowly, at rates of up to ten times slower than the aqueous solutions. This was probably because the presence of water on the SOA particles relied on uptake from the gas phase and because NH_4^+ was not present in excess. It needs to be stressed, then, that the estimated absorption coefficient represents an upper limit.

[34] The effective absorption Ångström exponent, α, for aged SOA can be obtained in the usual way, from a linear fit of the base-e logarithms of wavelength and absorption. Using this method, α is calculated to be $\sim$7 for fresh aqueous extracts of SOA and $\sim$4.7 for aged extracts (see auxiliary material Figure S7). The peak at 505 nm does not lend itself to this type of exponential fit; omitting this region from the aged SOA fit increased α to from 4.7 to 5.3. These values of the absorption Ångström exponents are at the upper end of the range of measurements from water soluble organic carbon extracted from atmospheric aerosol [*Hoffer et al.*, 2006; *Kirchstetter and Novakov*, 2004]. The apparent drop in α during aging is a direct result of a faster growth in visible absorption compared to the absorption in the near-UV range.

[35] The significance of this calculated aerosol absorption coefficient is clear when juxtaposed with measured coefficients from various regions. Absorption coefficients of rural aerosol in Hungary were measured to be $1-9 \times 10^{-6}$ m^{-1}, while for urban aerosol in Taipei $\beta = 33 \times 10^{-6}$ m^{-1} [*Chou et al.*, 2005; *Molnár and Mészáros*, 2001]. Based on these figures, $\beta = 0.06 \times 10^{-6}$ m^{-1} represents a fairly small but nonnegligible contribution to the total aerosol absorption. In rural areas or polluted tropical regions the contribution of aged SOA to the absorption could be significant; in urban and industrialized areas the absorbing aerosol is more likely to be dominated by elemental carbon.

[36] **Acknowledgments.** We acknowledge support provided by the NSF Atmospheric Chemistry program, ATM-0831518. The postdoctoral fellowship for David Bones was supported by the EMSI program, CHE-0431312. This work would not have been possible without facilities at the School of Physical Sciences, the AirUCI Institute, and the Urban Water Research Center at the University of California, Irvine. We thank Christopher D. Vanderwal for helpful discussion on the chemistry of pyridinium ions.

References

Andreae, M. O., and A. Gelencsér (2006), Black carbon or brown carbon? The nature of light-absorbing carbonaceous aerosols, *Atmos. Chem. Phys.*, *6*, 3131–3148.

Barsanti, K. C., and J. F. Pankow (2005), Thermodynamics of the formation of atmospheric organic particulate matter by accretion reactions—2. Dialdehydes, methylglyoxal, and diketones, *Atmos. Environ.*, *39*, 6597–6607, doi:10.1016/j.atmosenv.2005.07.056.

Bateman, A. P., et al. (2009), Time-resolved molecular characterization of limonene/ozone aerosol using high-resolution electrospray ionization mass spectrometry, *Phys. Chem. Chem. Phys.*, *11*(36), 7931–7942.

Bergstrom, R. W., Jr. (1972), Predictions of the spectral absorption and extinction coefficients of an urban air-pollution aerosol model, *Atmos. Environ.*, *6*, 247–258, doi:10.1016/0004-6981(72)90083-2.

Bergstrom, R. W., et al. (2002), Wavelength dependence of the absorption of black carbon particles: Predictions and results from the TARFOX experiment and implications for the aerosol single scattering albedo, *J. Atmos. Sci.*, *59*, 567–577, doi:10.1175/1520-0469(2002)059<0567:WDOTAO>2.0.CO;2.

Bergstrom, R. W., et al. (2007), Spectral absorption properties of atmospheric aerosols, *Atmos. Chem. Phys.*, *7*, 5937–5943.

Blough, N. V., and R. Del Vecchio (2002), Chromophoric DOM in the coastal environment, in *Biogeochemistry of Marine Dissolved Organic Matter*, edited by D. A. Hansell and C. A. Carlson, pp. 509–546, Academic Press, San Diego, Calif.

Casale, M. T., et al. (2007), Kinetics of acid-catalyzed aldol condensation reactions of aliphatic aldehydes, *Atmos. Environ.*, *41*, 6212–6224, doi:10.1016/j.atmosenv.2007.04.002.

Chen, J., and R. J. Griffin (2005), Modeling secondary organic aerosol formation from oxidation of α-pinene, β-pinene, and *d*-limonene, *Atmos. Environ.*, *39*, 7731–7744, doi:10.1016/j.atmosenv.2005.05.049.

Chio, K. S., and A. L. Tappel (1969), Synthesis and characterization of the fluorescent products derived from malonaldehyde and amino acids, *Biochemistry*, *8*, 2821–2827, doi:10.1021/bi00835a019.

Chou, C. C.-K., W.-N. Chen, S.-Y. Chang, T.-K. Chen, and S.-H. Huang (2005), Specific absorption cross-section and elemental carbon content of urban aerosols, *Geophys. Res. Lett.*, *32*, L21808, doi:10.1029/2005GL024301.

Corrigan, A. L., et al. (2008), Uptake of glyoxal by organic and inorganic aerosol, *Environ. Sci. Technol.*, *42*, 4428–4433, doi:10.1021/es7032394.
Czoschke, N. M., and M. Jang (2006a), Acidity effects on the formation of α-pinene ozone SOA in the presence of inorganic seed, *Atmos. Environ.*, *40*, 4370–4380, doi:10.1016/j.atmosenv.2006.03.030.
Czoschke, N. M., and M. Jang (2006b), Markers of heterogeneous reaction products in (-pinene ozone secondary organic aerosol, *Atmos. Environ.*, *40*, 5629–5639, doi:10.1016/j.atmosenv.2006.05.004.
Czoschke, N. M., et al. (2003), Effect of acidic seed on biogenic secondary organic aerosol growth, *Atmos. Environ.*, *37*, 4287–4299, doi:10.1016/S1352-2310(03)00511-9.
Debus, H. (1858), Über die einwirkung des ammoniaks auf glyoxal, *Justus Liebigs Ann. Chem.*, *107*, 199–208, doi:10.1002/jlac.18581070209.
De Haan, D. O., et al. (2009), Secondary organic aerosol-forming reactions of glyoxal with amino acids, *Environ. Sci. Technol.*, *43*, 2818–2824, doi:10.1021/es803534f.
Dinar, E., et al. (2008), The complex refractive index of atmospheric and model humic-like substances (HULIS) retrieved by a cavity ring down aerosol spectrometer (CRD-AS), *Faraday Discuss.*, *137*, 279–295, doi:10.1039/b703111d.
Duncan, J. L., et al. (1999), Chemistry at and near the surface of liquid sulfuric acid: A kinetic, thermodynamic and mechanistic analysis of heterogeneous reactions of acetone, *J. Phys. Chem. B*, *103*, 7247–7259, doi:10.1021/jp991322w.
Eisner, U., and J. Kuthan (1972), Chemistry of dihydropyridines, *Chem. Rev.*, *72*, 1–42, doi:10.1021/cr60275a001.
Forster, P., et al. (2007), Changes in atmospheric constituents and in radiative forcing, in *Climate Change 2007: The Physical Science Basis. Contribution of Working Group I to the Fourth Assessment Report of the Intergovernmental Panel on Climate Change*, edited by S. Solomon et al., pp. 747–845, Cambridge Univ. Press, Cambridge, U. K.
Galloway, M. M., et al. (2008), Glyoxal uptake on ammonium sulphate seed aerosol: Reaction products and reversibility of uptake under dark and irradiated conditions, *Atmos. Chem. Phys. Discuss.*, *8*, 20,799–20,838.
Galloway, M. M., et al. (2009), Glyoxal uptake on ammonium sulphate seed aerosol: Reaction products and reversibility of uptake under dark and irradiated conditions, *Atmos. Chem. Phys.*, *9*, 3331–3345.
Garland, R. M., et al. (2006), Acid-catalyzed reactions of hexanal on sulfuric acid particles: Identification of reaction products, *Atmos. Environ.*, *40*, 6863–6878, doi:10.1016/j.atmosenv.2006.07.009.
Gelencsér, A., et al. (2000), Structural characterization of organic matter in fine tropospheric aerosol by pyrolysis-gas chromatography-mass spectrometry, *J. Atmos. Chem.*, *37*, 173–183, doi:10.1023/A:1006402731340.
Gelencsér, A., A. Hoffer, Z. Krivácsy, G. Kiss, A. Molnár, and E. Mészáros (2002), On the possible origin of humic matter in fine continental aerosol, *J. Geophys. Res.*, *107*(D12), 4137, doi:10.1029/2001JD001299.
Gelencsér, A., et al. (2003), In-situ formation of light-absorbing organic matter in cloud water, *J. Atmos. Chem.*, *45*, 25–33, doi:10.1023/A:1024060428172.
Glasius, M., et al. (2000), Carboxylic acids in secondary aerosols from oxidation of cyclic monoterpenes by ozone, *Environ. Sci. Technol.*, *34*, 1001–1010, doi:10.1021/es990445r.
Graber, E. R., and Y. Rudich (2006), Atmospheric HULIS: How humic-like are they? A comprehensive and critical review, *Atmos. Chem. Phys.*, *6*, 729–753.
Griesbaum, K., et al. (1996), Ozonides of mono-, bi- and tricyclic terpenes, *Tetrahedron*, *52*, 14,813–14,826, doi:10.1016/0040-4020(96)00936-2.
Heaton, K. J., et al. (2007), Oligomers in the early stage of biogenic secondary organic aerosol formation and growth, *Environ. Sci. Technol.*, *41*, 6129–6136, doi:10.1021/es070314n.
Hodzic, A., et al. (2006), Aerosol chemical and optical properties over the Paris area within ESQUIF project, *Atmos. Chem. Phys.*, *6*, 3257–3280.
Hoffer, A., G. Kiss, M. Blazsó, and A. Gelencsér (2004), Chemical characterization of humic-like substances (HULIS) formed from a lignin-type precursor in model cloud water, *Geophys. Res. Lett.*, *31*, L06115, doi:10.1029/2003GL018962.
Hoffer, A., et al. (2006), Optical properties of humic-like substances (HULIS) in biomass-burning aerosols, *Atmos. Chem. Phys.*, *6*, 3563–3570.
Holmes, B. J., and G. A. Petrucci (2007), Oligomerization of levoglucosan by Fenton chemistry in proxies of biomass burning aerosols, *J. Atmos. Chem.*, *58*, 151–166, doi:10.1007/s10874-007-9084-8.
Horvath, H. (1993), Atmospheric light-absorption—A review, *Atmos. Environ., Part A*, *27*, 293–317, doi:10.1016/0960-1686(93)90104-7.
Iinuma, Y., et al. (2004), Aerosol-chamber study of the α-pinene/O_3 reaction: Influence of particle acidity on aerosol yields and products, *Atmos. Environ.*, *38*, 761–773, doi:10.1016/j.atmosenv.2003.10.015.
Jacobson, M. Z. (1999), Isolating nitrated and aromatic aerosols and nitrated aromatic gases as sources of ultraviolet light absorption, *J. Geophys. Res.*, *104*, 3527–3542, doi:10.1029/1998JD100054.
Jang, M., et al. (2002), Heterogeneous atmospheric aerosol production by acid-catalyzed particle-phase reactions, *Science*, *298*, 814–817, doi:10.1126/science.1075798.
Jaoui, M., et al. (2006), Analysis of secondary organic aerosol compounds from the photooxidation of *d*-limonene in the presence of NO_x and their detection in ambient $PM_{2.5}$, *Environ. Sci. Technol.*, *40*, 3819–3828, doi:10.1021/es052566z.
Jonsson, Å. M., et al. (2008), Influence of OH scavenger on the water effect on Secondary Organic Aerosol formation from ozonolysis of limonene, Δ^3-carene, and α-pinene, *Environ. Sci. Technol.*, *42*, 5938–5944, doi:10.1021/es702508y.
Kanakidou, M., et al. (2005), Organic aerosol and global climate modelling: A review, *Atmos. Chem. Phys.*, *5*, 1053–1123.
Katritzky, A. R., et al. (1986), The mechanism of the Hantzsch pyridine synthesis: A study by ^{15}N and ^{13}C NMR spectroscopy, *Tetrahedron*, *42*, 5729–5738, doi:10.1016/S0040-4020(01)88178-3.
Kieber, R. J., et al. (2006), Chromophoric Dissolved Organic Matter (CDOM) in rainwater, southeastern North Carolina, USA, *J. Atmos. Chem.*, *54*, 21–41, doi:10.1007/s10874-005-9008-4.
Kirchstetter, T. W., and T. Novakov (2004), Evidence that the spectral dependence of light absorption by aerosols is affected by organic carbon, *J. Geophys. Res.*, *109*, D21208, doi:10.1029/2004JD004999.
Kroll, J. H., and J. H. Seinfeld (2008), Chemistry of secondary organic aerosol: Formation and evolution of low-volatility organics in the atmosphere, *Atmos. Environ.*, *42*, 3593–3624, doi:10.1016/j.atmosenv.2008.01.003.
Kroll, J. H., N. L. Ng, S. M. Murphy, V. Varutbangkul, R. C. Flagan, and J. H. Seinfeld (2005), Chamber studies of secondary organic aerosol growth by reactive uptake of simple carbonyl compounds, *J. Geophys. Res.*, *110*, D23207, doi:10.1029/2005JD006004.
Kua, J., et al. (2008), Thermodynamics and kinetics of glyoxal dimer formation: A computational study, *J. Phys. Chem. A*, *112*, 66–72, doi:10.1021/jp076573g.
Kwamena, N.-O. A., and J. P. D. Abbatt (2008), Heterogeneous nitration reactions of polycyclic aromatic hydrocarbons and n-hexane soot by exposure to $NO_3/NO_2/N_2O_5$, *Atmos. Environ.*, *42*, 8309–8314, doi:10.1016/j.atmosenv.2008.07.037.
Larsen, B. R., et al. (1998), Atmospheric oxidation products of terpenes: A new nomenclature, *Chemosphere*, *37*, 1207–1220, doi:10.1016/S0045-6535(98)00115-5.
Lawrence, S. A. (2004), *Amines*, Cambridge Univ. Press, Cambridge, U. K.
Leungsakul, S., et al. (2005), Kinetic mechanism for predicting secondary organic aerosol formation from the reaction of d-limonene with ozone, *Environ. Sci. Technol.*, *39*, 9583–9594, doi:10.1021/es0492687.
Li, Y. J., et al. (2008), Accretion reactions of octanal catalyzed by sulfuric acid: Product identification, reaction pathways, and atmospheric implications, *Environ. Sci. Technol.*, *42*, 7138–7145, doi:10.1021/es7031373.
Liggio, J., S.-M. Li, and R. McLaren (2005), Reactive uptake of glyoxal by particulate matter, *J. Geophys. Res.*, *110*, D10304, doi:10.1029/2004JD005113.
Limbeck, A., M. Kulmala, and H. Puxbaum (2003), Secondary organic aerosol formation in the atmosphere via heterogeneous reaction of gaseous isoprene on acidic particles, *Geophys. Res. Lett.*, *30*(19), 1996, doi:10.1029/2003GL017738.
Lukács, H., et al. (2007), Seasonal trends and possible sources of brown carbon based on 2-year aerosol measurements at six sites in Europe, *J. Geophys. Res.*, *112*, D23S18, doi:10.1029/2006JD008151.
Mang, S. A., et al. (2008), Contribution of carbonyl photochemistry to aging of atmospheric secondary organic aerosol, *J. Phys. Chem. A*, *112*, 8337–8344, doi:10.1021/jp804376c.
Marley, N. A., et al. (2009), The impact of biogenic carbon sources on aerosol absorption in Mexico City, *Atmos. Chem. Phys.*, *9*, 1537–1549.
Molnár, A., and E. Mészáros (2001), On the relation between the size and chemical composition of aerosol particles and their optical properties, *Atmos. Environ.*, *35*, 5053–5058, doi:10.1016/S1352-2310(01)00314-4.
Moosmüller, H., et al. (2009), Aerosol light absorption and its measurement: A review, *J. Quant. Spectrosc. Radiat. Transfer*, *110*, 844–878, doi:10.1016/j.jqsrt.2009.02.035.
Mukai, H., and Y. Ambe (1986), Characterization of a humic acid-like brown substance in airborne particulate matter and tentative identification of its origin, *Atmos. Environ.*, *20*, 813–819, doi:10.1016/0004-6981(86)90265-9.
Ng, N. L., et al. (2006), Contribution of first- versus second-generation products to secondary organic aerosols formed in the oxidation of biogenic hydrocarbons, *Environ. Sci. Technol.*, *40*, 2283–2297, doi:10.1021/es052269u.
Nozière, B., and A. Córdova (2008), A kinetic and mechanistic study of the amino acid catalyzed aldol condensation of acetaldehyde in aqueous and salt solutions, *J. Phys. Chem. A*, *112*, 2827–2837, doi:10.1021/jp7096845.

Nozière, B., and W. Esteve (2005), Organic reactions increasing the absorption index of atmospheric sulfuric acid aerosols, *Geophys. Res. Lett.*, *32*, L03812, doi:10.1029/2004GL021942.

Nozière, B., P. Dziedzic, and A. Córdova (2007), Formation of secondary light-absorbing "fulvic-like" oligomers: A common process in aqueous and ionic atmospheric particles?, *Geophys. Res. Lett.*, *34*, L21812, doi:10.1029/2007GL031300.

Nozière, B., et al. (2009a), Common inorganic ions are efficient catalysts for organic reactions in atmospheric aerosols and other natural environments, *Atmos. Chem. Phys. Discuss.*, *9*, 1–21.

Nozière, B., et al. (2009b), Products and kinetics of the liquid-phase reaction of glyoxal catalyzed by ammonium ions (NH_4^+), *J. Phys. Chem. A*, *113*, 231–237, doi:10.1021/jp8078293.

Peltier, R. E., A. P. Sullivan, R. J. Weber, A. G. Wollny, J. S. Holloway, C. A. Brock, J. A. de Gouw, and E. L. Atlas (2007), No evidence for acid-catalyzed secondary organic aerosol formation in power plant plumes over metropolitan Atlanta, Georgia, *Geophys. Res. Lett.*, *34*, L06801, doi:10.1029/2006GL028780.

Pitts, J. N., et al. (1978), Atmospheric reactions of polycyclic aromatic hydrocarbons: Facile formation of mutagenic nitro derivatives, *Science*, *202*, 515–519, doi:10.1126/science.705341.

Reid, J. S., et al. (2005), A review of biomass burning emissions part II: Intensive physical properties of biomass burning particles, *Atmos. Chem. Phys.*, *5*, 799–825.

Roden, C., et al. (2006), Emission factors and real-time optical properties of particles emitted from traditional wood burning cookstoves, *Environ. Sci. Technol.*, *40*, 6750–6757, doi:10.1021/es052080i.

Rudich, Y., et al. (2007), Aging of organic aerosol: Bridging the gap between laboratory and field studies, *Annu. Rev. Phys. Chem.*, *58*, 321–352, doi:10.1146/annurev.physchem.58.032806.104432.

Santos, P. S. M., et al. (2009), Spectroscopic characterization of dissolved organic matter isolated from rainwater, *Chemosphere*, *74*, 1053–1061, doi:10.1016/j.chemosphere.2008.10.061.

Shapiro, E. L., et al. (2009), Light-absorbing secondary organic material formed by glyoxal in aqueous aerosol mimics, *Atmos. Chem. Phys.*, *9*, 2289–2300.

Shilling, J. E., et al. (2009), Loading-dependent elemental composition of α-pinene SOA particles, *Atmos. Chem. Phys.*, *9*, 771–782.

Tolocka, M. P., et al. (2004), Formation of oligomers in secondary organic aerosol, *Environ. Sci. Technol.*, *38*, 1428–1434, doi:10.1021/es035030r.

Tsigaridis, K., et al. (2006), Change in global aerosol composition since preindustrial times, *Atmos. Chem. Phys.*, *6*, 5143–5162.

Volkamer, R., F. San Martini, L. T. Molina, D. Salcedo, J. L. Jimenez, and M. J. Molina (2007), A missing sink for gas-phase glyoxal in Mexico City: Formation of secondary organic aerosol, *Geophys. Res. Lett.*, *34*, L19807, doi:10.1029/2007GL030752.

Walser, M. L., et al. (2008), High-resolution mass spectrometric analysis of secondary organic aerosol produced by ozonation of limonene, *Phys. Chem. Chem. Phys.*, *10*, 1009–1022, doi:10.1039/b712620d.

Yang, M., et al. (2009), Attribution of aerosol light absorption to black carbon, brown carbon, and dust in China—Interpretations of atmospheric measurements during EAST-AIRE, *Atmos. Chem. Phys.*, *9*, 2035–2050.

Zappoli, S., et al. (1999), Inorganic, organic and macromolecular components of fine aerosol in different areas of Europe in relation to their water solubility, *Atmos. Environ.*, *33*, 2733–2743, doi:10.1016/S1352-2310(98)00362-8.

Zepp, R. G., et al. (2004), Dissolved organic fluorophores in southeastern US coastal waters: Correction method for eliminating Rayleigh and Raman scattering peaks in excitation-emission matrices, *Mar. Chem.*, *89*, 15–36, doi:10.1016/j.marchem.2004.02.006.

Zhang, D., et al. (2002), Mechanism of OH formation from ozonolysis of isoprene: Kinetics and product yields, *Chem. Phys. Lett.*, *358*, 171–179, doi:10.1016/S0009-2614(02)00260-9.

Zhang, J., et al. (2006), Secondary organic aerosol formation from limonene ozonolysis: Homogeneous and heterogeneous influences as a function of NO_x, *J. Phys. Chem. A*, *110*, 11,053–11,063, doi:10.1021/jp062836f.

Zhao, J., N. P. Levitt, and R. Zhang (2005), Heterogeneous chemistry of octanal and 2,4-hexadienal with sulfuric acid, *Geophys. Res. Lett.*, *32*, L09802, doi:10.1029/2004GL022200.

A. P. Bateman, D. L. Bones, D. K. Henricksen, S. A. Mang, T. B. Nguyen, and S. A. Nizkorodov, Department of Chemistry, University of California, Irvine, CA 92697, USA. (nizkorod@uci.edu)

W. J. Cooper and M. Gonsior, Department of Civil and Environmental Engineering, University of California, Irvine, CA 92697, USA.